

Breaking the Euclidean Barrier: Hyperboloid-Based Biological Sequence Analysis

Sarwan Ali^{1*}, Haris Mansoor³ and Murray Patterson²

¹Department Of Neurology, Columbia University, New York, 10032, NY, USA.

²Department Of Computer Science, Georgia State University, Atlanta, 30302, Georgia, USA.

³Department Of Computer Science, Lahore University of Management Sciences (LUMS), Lahore, Pakistan.

*Corresponding author(s). E-mail(s): sa4559@cumc.columbia.edu;
Contributing authors: 16060061@lums.edu.pk;
mpatterson30@gsu.edu;

Abstract

Genomic sequence analysis plays a crucial role in various scientific and medical domains. Traditional machine-learning approaches often struggle to capture the complex relationships and hierarchical structures of sequence data when working in high-dimensional Euclidean spaces. This limitation hinders accurate sequence classification and similarity measurement. To address these challenges, this research proposes a method to transform the feature representation of biological sequences into the hyperboloid space. By applying a transformation, the sequences are mapped onto the hyperboloid, preserving their inherent structural information. Once the sequences are represented in the hyperboloid space, a kernel matrix is computed based on the hyperboloid features. The kernel matrix captures the pairwise similarities between sequences, enabling more effective analysis of biological sequence relationships. This approach leverages the inner product of the hyperboloid feature vectors to measure the similarity between pairs of sequences. The experimental evaluation of the proposed approach demonstrates its efficacy in capturing important sequence correlations and improving classification accuracy.

Keywords: Bio-sequence Analysis, Sequence Classification, k-mers, Spike Sequence, Feature Vector Representation

1 Introduction

The analysis of biological sequences is a fundamental task in bioinformatics, enabling us to comprehend the structure, function, and evolution of biological molecules [1, 2]. Recent progress in machine learning and artificial intelligence has paved the way for learning representations of symbolic data, including text, graphs, and multi-relational data [3–6]. In the realm of biological sequence analysis, understanding the characteristics and relationships of sequences is crucial, particularly in genomics, where the examination of genetic or protein sequences provides valuable insights into biological functions [7, 8]. Nevertheless, conventional machine learning approaches encounter limitations in capturing the intricate relationships and hierarchical structures inherent in genomic sequences due to the high-dimensional Euclidean spaces they operate within.

In the realm of protein sequences, three types of structures are associated with them: Primary, Secondary, and Tertiary Structures [9]. The primary structure refers to the linear sequence of amino acids comprising the protein chain, while the secondary structure encompasses the local folding patterns and regular repeating structures within the chain. Furthermore, the tertiary structure represents the overall three-dimensional arrangement of the protein molecule.

Hierarchical and tree-like structures are inherent in biological sequences and play a crucial role in understanding the evolutionary processes across species. Phylogenetic trees have been traditionally used to capture these structures and explain the relationships between sequences [10]. However, constructing phylogenetic trees can be computationally intensive and may not be practical for large-scale sequence analysis. Additionally, even if a tree structure is available, calculating Euclidean distance directly from sequence embeddings can result in the loss of important structural information within the biological sequences. Unfortunately, when using Euclidean distance, the preservation of structural information is not achieved.

The adoption of machine learning (ML) models as alternatives to traditional methods has gained popularity due to their ease of use, generalizability, and efficient performance. However, a limitation of many ML models is their reliance on Euclidean distance computations, which leads to the loss of important structural information, such as the Primary, Secondary, and Tertiary Structures, when comparing numerical embeddings of biological sequences.

In recent years, several methods have been proposed for designing embeddings of biological sequences, including popular techniques such as one-hot encoding (OHE)[11] and the k -mers spectrum[12–16]. OHE-based embeddings suffer from high dimensionality and the loss of order information in amino acids/nucleotides within the sequences [17]. On the other hand, the k -mers spectrum can preserve the order of amino acids/nucleotides and capture aspects of the primary structure as well as other protein structures [18]. However, using Euclidean distance to compare

pairs of k -mers spectra fails to consider the structural information, limiting the performance of tasks like classification [19–22]. Furthermore, Euclidean distance often fails to capture the complex and nonlinear relationships inherent in sequence data. Consequently, there is a need for innovative approaches that can provide more effective and meaningful measures for comparing sequences [23–25]. One alternative to directly working with embeddings is the use of a kernel matrix [26], which projects the data into a higher-dimensional space by taking the dot product between the spectra of biological sequences [26]. However, this approach may not adequately capture all the nonlinear relationships and similarities between data points.

In order to overcome the challenges associated with the complex structures of biological sequences, this study introduces a novel approach that involves transforming the feature representation of these sequences into the hyperboloid space. By applying this transformation, the inherent structural information of the sequences is preserved as they are mapped onto the hyperboloid. The method consists of two steps: first, the conversion of the biological sequences into numerical form using the k -mers spectrum, and second, the transformation of the resulting spectra into corresponding hyperboloid feature vectors. This innovative approach shows great potential in capturing the intricate structural properties of biological sequences. Once the sequences are represented in the hyperboloid space, a kernel matrix is computed based on the hyperboloid features. This kernel matrix effectively captures the pairwise similarities between sequences, enabling a more meaningful analysis of the relationships among biological sequences. The approach leverages the inner product of the hyperboloid feature vectors as a measure of similarity between pairs of sequences.

One of the primary advantages of utilizing the hyperboloid space is its ability to preserve the hierarchical and tree-like structures inherent in biological sequences. Unlike Euclidean representations, which often overlook these intricate relationships, the hyperboloid space provides a more accurate representation that captures the complex dependencies among sequences. Furthermore, the proposed method overcomes the limitations of Euclidean spaces by preserving the structural information of the sequences, including their three-dimensional arrangements (tertiary structure) and hidden hierarchical relationships.

Our contributions in this paper are the following:

1. We propose a novel approach that transforms the feature representation of biological sequences into the hyperboloid space, preserving their inherent structural information.
2. Computation of a kernel matrix based on the hyperboloid features, capturing pairwise similarities between sequences and enabling more effective analysis of biological sequence relationships.
3. We also provide theoretical analysis for the designed embeddings.
4. Experimental evaluation demonstrating the efficacy of the proposed approach in capturing important sequence correlations and improving classification accuracy.

The subsequent sections of this paper are structured as follows: Section 2 presents a comprehensive review of the relevant literature pertaining to the proposed method.

4 *Breaking the Euclidean Barrier*

The contribution of this paper is outlined and discussed in Section 3. Details regarding the dataset statistics and experimental setup are provided in Section 4. The results obtained from the proposed and baseline models are presented and analyzed in Section 5. Lastly, Section 6 concludes this study by summarizing the key findings and implications.

2 Related Work

In this section, we provide a comprehensive review of the existing literature and approaches in the field of biological sequence analysis, focusing on distance measures. We discuss the strengths and limitations of traditional methods and identify the specific gaps that our proposed approach aims to overcome.

Traditional distance measures, including Euclidean distance [27], Hamming distance [28], and cosine similarity [29], have been widely utilized in biological sequence analysis. These measures assume that sequences can be represented as vectors in a Euclidean space [30–32]. While they have demonstrated effectiveness in certain applications, they exhibit limitations when applied to sequences with intricate structures and dependencies [32]. For instance, Euclidean distance fails to capture the hierarchical relationships and tree-like structures that are common in many sequence datasets. Additionally, these measures often encounter challenges when dealing with high-dimensional sequence data and may yield suboptimal results [33].

Graph-based approaches have garnered significant attention in sequence analysis due to their capacity to capture intricate relationships and dependencies. These methods construct a graph where each sequence corresponds to a node, and nodes are connected by edges if they exhibit a certain level of similarity, commonly referred to as a k -nearest neighbor (k NN) graph [34]. Additionally, in protein-protein interaction networks, edges can be formed based on the binding interactions between specific proteins [35]. However, these approaches can be computationally demanding and may encounter difficulties when dealing with large-scale sequence datasets. Furthermore, it remains unclear from the literature whether these methods can effectively capture diverse hierarchical and structural information inherent in biological sequences (e.g., the potential loss of information when constructing a k NN graph based on Euclidean distance).

Embedding-based methods seek to map sequences into low-dimensional vector spaces, where the similarity between biological sequences is reflected in the distances between embeddings [36–38]. Approaches such as k -mers spectrum [12, 17, 39] have demonstrated promising performance in supervised and unsupervised tasks. However, these methods often suffer from computational complexity or face challenges in preserving the hierarchical and structural relationships inherent in sequences.

Generating a kernel or gram matrix has become a popular approach for calculating the pairwise similarity between sequences, offering an alternative to traditional embedding methods [17]. However, the computational cost associated with computing pairwise similarities can be significant. To mitigate this challenge, researchers in [26] proposed an approximate method that enhances the efficiency of kernel computation. Their approach involves evaluating the dot product between the spectra of

two sequences. The resulting kernel matrix can then be employed as input for kernel classifiers, such as Support Vector Machines (SVM), or non-kernel classifiers utilizing kernel PCA [40], for classification tasks [17]. Despite these advancements, these methods still encounter difficulties in capturing the underlying hierarchical and structural information intrinsic to biological sequences.

In recent years, there has been growing interest in leveraging hyperbolic geometry for sequence analysis [32, 41]. Hyperbolic space possesses unique properties that make it particularly suitable for capturing hierarchical and tree-like structures [32]. Previous studies have demonstrated the effectiveness of hyperbolic representations in various tasks, including text classification [42], network analysis [43], and knowledge graph embeddings [44]. However, the application of hyperbolic geometry to biological sequence analysis remains relatively unexplored, highlighting the need for specialized distance measures that harness the advantages of hyperbolic space for the classification of biological sequences.

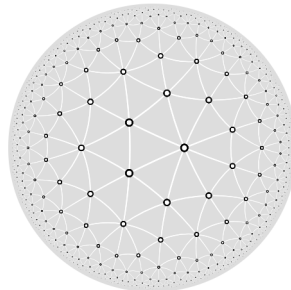


Fig. 1: Hyperboloid isosceles tiling, each triangle has two equal sides and equal angles, we can observe negative curvature and exponential growth.

3 Proposed Approach

Given an vector space $\mathcal{X} \in \mathbb{R}^{n+1}$ (e.g., proteins, etc.), function : $\mathcal{X} \times \mathcal{X} \rightarrow \mathbb{R}$ is called a kernel function. Kernel functions are used to quantify the similarity between a pair of objects $X, Y \in \mathcal{X}$. We propose a kernel function in hyperbolic geometry. Hyperbolic geometry is a non-Euclidean geometry that studies space of constant negative curvature. The underlying hyperbolic geometry allows us to learn similarity better than Euclidean space.

Input Embedding Representation

In this study, we employ the k -mers spectrum [17] as the input for our model. The k -mers spectrum represents sequences by capturing the frequency of all possible subsequences of length k , where $k > 0$. It provides a concise encoding of sequences by incorporating the frequencies of all possible k -mers. Compared to other encoding schemes like one-hot encoding (OHE) [11], the k -mers spectrum offers several advantages. OHE suffers from high dimensionality and sparsity, particularly for large

6 *Breaking the Euclidean Barrier*

alphabets or long sequences. In contrast, the k -mers spectrum preserves positional and contextual information within the sequence. It takes into account the occurrence and frequencies of subsequences, enabling the detection of patterns, motifs, and dependencies within the sequence, which are crucial for various sequence analysis tasks.

Remark 1 We also experimented with the one-hot encoding-based representation of biological sequences as input for the proposed methods. However, the results were not promising compared to the k -mers-based spectrum, primarily due to the reasons discussed above. Therefore, we have not included those results in this paper.

We divide our method into two steps: we first compute the pairwise distance between the data points in hyperbolic space. In the second step, we use kernel PCA to get the final embeddings, which are then used for the underlying supervised analysis.

3.1 Hyperboloid Model

In geometry, the hyperboloid model is a model of n -dimensional geometry in which points are represented on the forward sheet S^+ of a two-sheeted hyperboloid in $(n + 1)$ -dimensional Minkowski space or by the displacement vectors from the origin to those points. In the hyperboloid model, m -dimensional subspaces (m -planes) are formed by intersecting the forward sheet S^+ with $(m + 1)$ -dimensional hyperplanes in Minkowski space that pass through the origin. Alternatively, these can be constructed using the exterior (wedge) product of m displacement vectors from the origin. Similar to how spherical distance is inherited from Euclidean distance when the n -sphere is embedded in $(n + 1)$ -dimensional Euclidean space, hyperbolic space is embedded isometrically in Minkowski space. The same ideas (such as points, lines, angles, and circles) can be applied to hyperbolic geometry when they are transferred to the forward sheet of a hyperboloid. Representing data in hyperbolic space has an intrinsic advantage as many natural processes have a structure better suited for hyperbolic space. This is because many phenomena have an exponential relationship, which becomes evident in hyperbolic space.

Figure 1 shows a visualization of a particular type of tiling (isosceles) in hyperbolic geometry. In a hyperbolic isosceles tiling, the tiles used are hyperbolic isosceles triangles: they have two equal sides and angles. These triangles are created by cutting a hyperbolic plane into congruent triangles, each having two sides of the same length.

Let $X = (x_0, x_1 \cdots x_n)$ and $Y = (y_0, y_1 \cdots y_n)$ be two points on the positive hyperbolic sheet, the distance between X and Y is given by:

$$d(X, Y) = \cosh^{-1}(B(X, Y)) \quad (1)$$

where,

$$B(X, Y) = x_0y_0 - x_1y_1 - x_2y_2 - \cdots - x_ny_n \quad (2)$$

The domain of Equation 1 is $B(X, Y) \geq 1$, where $\cosh^{-1}(1) = 0$ (corresponding to identical points) and $\cosh^{-1}(B(X, Y)) > 0$ for $B(X, Y) > 1$. The expression

$d(X, Y)$ can serve as a kernel function in hyperbolic space. A kernel function typically satisfies the following two properties: non-negativity, and symmetry. A kernel with these properties will loosely have the interpretation as a similarity quantification; that is $d(X, Y)$ represents a similarity metric on input space.

- **Non-Negativity:** $d(X, Y) > 0$
- **Symmetry:** $d(X, Y) = d(Y, X)$

The expression $B(X, Y) = x_0 y_0 - \sum_{i=1}^n x_i y_i$ represents the Lorentzian inner product $\langle X, Y \rangle_L$ in Minkowski space satisfying $\langle X, X \rangle_L = x_0^2 - \sum_{i=1}^n x_i^2 = 1$ (with $x_0 > 0$) and similarly for Y .

Proof:

Let $p = \|\vec{x}\| = \sqrt{\sum_{i=1}^n x_i^2}$, so $x_0 = \sqrt{1 + p^2}$. Similarly, let $q = \|\vec{y}\|$, so $y_0 = \sqrt{1 + q^2}$. Then,

$$B(X, Y) = x_0 y_0 - \vec{x} \cdot \vec{y} \geq x_0 y_0 - \|\vec{x}\| \|\vec{y}\| = \sqrt{1 + p^2} \sqrt{1 + q^2} - pq,$$

where the inequality holds by the (standard) Cauchy-Schwarz inequality on the spatial Euclidean vectors \vec{x} and \vec{y} , with equality when \vec{x} and \vec{y} are parallel. It remains to show that the lower bound $f(p, q) = \sqrt{1 + p^2} \sqrt{1 + q^2} - pq \geq 1$. Rationalize the expression:

$$f(p, q) = \frac{(1 + p^2)(1 + q^2) - (pq)^2}{\sqrt{1 + p^2} \sqrt{1 + q^2} + pq} = \frac{1 + p^2 + q^2}{\sqrt{1 + p^2} \sqrt{1 + q^2} + pq}.$$

To verify $f(p, q) \geq 1$:

- At $p = q = 0$, $f(0, 0) = 1$.
- For $p = q$, $f(p, p) = \frac{1+2p^2}{1+p^2+p^2} = \frac{1+2p^2}{1+2p^2} = 1$.
- For unequal values, e.g., $q = 0$, $f(p, 0) = \sqrt{1 + p^2} > 1$ for $p > 0$.

The minimum value of 1 occurs when $p = q$ and the spatial vectors are aligned (corresponding to $X = Y$); otherwise, $B(X, Y) > 1$. This confirms the domain condition for $\cosh^{-1}(B(X, Y))$.

since,

$$\cosh^{-1}(z) = \ln \left(z + \sqrt{z^2 - 1} \right) \quad 1 \leq z < \infty \quad (3)$$

Using the Taylor series expansion of \ln

$$\ln(z) = (z - 1) - \frac{(z - 1)^2}{2} + \frac{(z - 1)^3}{3} - \frac{(z - 1)^4}{4} + \dots \quad (4)$$

Taylor series expansion of $\cosh^{-1}(z)$ around 1 is given below

$$\begin{aligned} \cosh^{-1}(z) &= (z - 1 + \sqrt{z^2 - 1}) \\ &- \frac{(z - 1 + \sqrt{z^2 - 1})^2}{2} + \frac{(z - 1 + \sqrt{z^2 - 1})^3}{3} \\ &- \frac{(z - 1 + \sqrt{z^2 - 1})^4}{4} \dots \end{aligned} \quad (5)$$

Using binomial expansion the above expression can be simplified into

$$\begin{aligned} \cosh^{-1}(z) &= (2z - 1 - \frac{1}{2z} - \frac{1}{8z^3} - \frac{1}{32z^5} \dots) - \\ &\frac{1}{2}(2z - 1 - \frac{1}{2z} - \frac{1}{8z^3} - \frac{1}{32z^5} \dots)^2 + \\ &\frac{1}{3}(2z - 1 - \frac{1}{2z} - \frac{1}{8z^3} - \frac{1}{32z^5} \dots)^3 + \dots \end{aligned} \quad (6)$$

Thus $d(X, Y)$ as a kernel map inputs to infinite dimensional polynomial feature space with both negative and positive exponents. The above expansions demonstrate that $d(X, Y)$ can be expressed as an infinite series resembling a polynomial kernel, allowing it to map inputs implicitly to a high-dimensional feature space. This means that the hyperboloid kernel effectively corresponds to a polynomial kernel of infinite degree. Polynomial kernels are well known for their ability to approximate complex nonlinear decision boundaries:

- Low-degree terms capture simple linear and quadratic patterns.
- High-degree terms represent increasingly intricate interactions between input features.

The pseudocode for computing the Hyperboloid kernel is given in Algorithm 1 and the flow chart is provided in Figure 2. The algorithm takes a set of biological sequences as input and computes k -mers spectrum-based numerical embeddings (line 1). It then iterates for all pairs of embeddings (upper triangle only due to symmetry property) and computes the Hyperboloid distance using Equation 1 and Equation 2 (line 7). The kernel matrix is further processed to kernel-PCA and then used in classification algorithms.

3.2 Theoretical Proof

Mercer's theorem, as discussed by [45], offers a fundamental underpinning for the utilization of kernel methods in machine learning. The theorem establishes that any positive semi-definite kernel function can be represented as the inner product of two functions in a feature space of high dimensionality. This enables us to bypass the explicit computation of the high-dimensional feature space and instead operate directly with the kernel function in the input space. Meeting the conditions of Mercer's theorem allows for the application of kernel methods like support vector machines (SVMs) and kernel principal component analysis (KPCA). These methods

bring forth advantages such as efficient computation, the flexibility to model intricate relationships between data, and the ability to handle non-linearly separable data. Additionally, the desirable properties of positive definiteness and full rank, which will be discussed in detail below, offer further benefits such as facilitating the construction of a reproducible kernel Hilbert Space (RKHS). This framework provides a basis for a unique and reproducible Kernel.

A kernel function $d(X_i, X_j) \forall X_i, x_j \in \mathbb{R}^n$ is called a Mercer kernel if it satisfies the following properties:

1. $d(X_i, X_j)$ is symmetric, i.e. $d(X_i, X_j) = d(X_j, X_i) \forall X_i$ and X_j .
2. For any set of data points X_1, X_2, \dots, X_n , the kernel matrix D defined by $D_{ij} = d(X_i, X_j)$ is positive semi-definite.

To prove this, let's consider the following conditions:

Symmetry:

The Hyperboloid kernel function is symmetric since,

$$d(X_i, X_j) = d(X_j, X_i) \quad (7)$$

The Hyperboloid kernel function is symmetric because:

$$B(X, Y) = x_0 y_0 - \sum_{i=1}^n x_i y_i \quad (8)$$

$$= y_0 x_0 - \sum_{i=1}^n y_i x_i = B(Y, X) \quad (9)$$

Since $B(X, Y) = B(Y, X)$, it immediately follows that:

$$d(X, Y) = \cosh^{-1}(B(X, Y)) = \cosh^{-1}(B(Y, X)) = d(Y, X) \quad (10)$$

Positive Semi Definite (PSD) Analysis:

The kernel matrix $\mathbf{D} \in \mathbb{R}^{n \times n}$ is defined as $D_{ij} = d(X_i, X_j)$ for all data points X_1, X_2, \dots, X_n in our dataset. To verify positive semi-definiteness (PSD), we must show that for any vector $\mathbf{v} \in \mathbb{R}^n$, the quadratic form $\mathbf{v}^T \mathbf{D} \mathbf{v} \geq 0$.

$$\mathbf{v}^T \mathbf{D} \mathbf{v} = \sum_{i=1}^n \sum_{j=1}^n v_i v_j D_{ij} = \sum_{i=1}^n \sum_{j=1}^n v_i v_j d(X_i, X_j) \quad (11)$$

Equation 11 follows directly from the definition of matrix multiplication:

$$\mathbf{v}^T \mathbf{D} \mathbf{v} = \sum_{i=1}^n v_i^2 d(X_i, X_i) + \sum_{i,j=1; i \neq j}^n v_i v_j d(X_i, X_j) \quad (12)$$

Equation 12 separates the diagonal terms ($i = j$) from the off-diagonal terms ($i \neq j$):

$$\sum_{i=1}^n v_i^2 d(X_i, X_i) \geq - \sum_{i,j=1; i \neq j}^n v_i v_j d(X_i, X_j) \quad (13)$$

We can add a positive number in $d(X_i, X_i)$ such that the inequality in the above equation is always satisfied. This has no effect on machine learning algorithms as these algorithms utilize the pairwise kernel measure for $i \neq j$. Thus, adding a positive number in $d(X_i, X_i)$ will make the kernel positive semidefinite without affecting the results.

Since the Hyperboloid function is a Mercer kernel, there exists a function ϕ that maps X_i, X_j into another space (possibly with much higher dimensions) such that

$$d(X_i, X_j) = \phi(X_i)^T \phi(X_j) \quad (14)$$

where, we can use d as a kernel since we know ϕ exists, even if we do not know what ϕ is. We can use $\phi(X_i)^T \phi(X_j)$ as a comparison metric between samples. In a number of machine learning and statistical models, the feature vector X only enters the model through comparisons with other feature vectors. If we kernelize these inner products, When we are allowed to compute only $d(X_i, X_j)$ in computation and avoid working in feature space, we work in an $n \times n$ space (the Kernel matrix).

Algorithm 1 Hyperboloid Kernel Matrix

Input: Set of Biological Sequences n
Output: Hyperboloid kernel matrix K

```

1: embed ← KMERSPECTRUM(n)                                ▷ Using method from [17]
2: K ← np.zeros(|n|, |n|)
3: Initialize kernel matrix  $K$  with zeros
4: for  $i$  in range(n) do                                ▷ for all embeddings  $i$ 
5:   for  $j$  in range(n) do                                ▷ for all embeddings  $j$ 
6:     if  $i \leq j$  then
7:       kernel ←  $\cosh^{-1}(\text{embed}[i], \text{embed}[j])$     ▷ using Eq. 1 and Eq. 2
8:       Set  $K[i, j] = \text{kernel}$ 
9:       Set  $K[j, i] = K[i, j]$ 
10:    end if
11:   end for
12: end for
13: Return  $K$ 

```

3.3 Kernel PCA [40]

Once the kernel matrix is generated, we can utilize kernel PCA (Principal Component Analysis) to obtain a low-dimensional embedding of the sequences. PCA is a

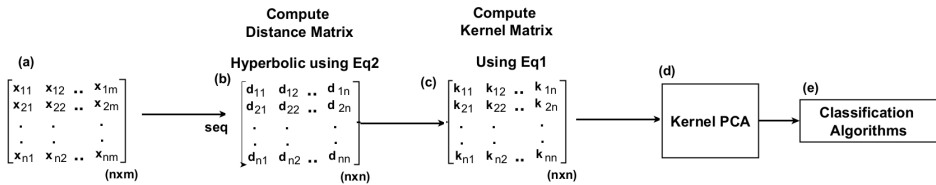


Fig. 2: Workflow for Hyperboloid Distance-based classification. Each row of the input matrix (a) represents a sequence vector computed using k -mers spectrum. The sequence is first converted into kernel matrix using hyperboloid distance (b) and (c), then the kernel matrix is processed through Kernel-PCA (d) and used in the classification algorithms.

dimensionality reduction technique that finds a set of orthogonal axes (principal components) along which the data exhibits the most variation. Kernel PCA extends this method to nonlinear data by using the kernel matrix to implicitly map the data into a high-dimensional feature space.

In kernel PCA, the principal components are computed based on the eigenvectors of the kernel matrix rather than the original data. This allows for the discovery of patterns and structures in the data. The resulting low-dimensional embeddings, also known as kernel principal components, capture the essential information while preserving the nonlinear relationships among the sequences.

By applying kernel PCA to the kernel matrix generated from the hyperboloid distance, we can obtain a reduced-dimensional representation of the sequences. This representation can be used for various downstream tasks, such as clustering, classification, or visualization, where the nonlinear structure of the data is important.

The advantage of using kernel PCA with the Hyperboloid distances lies in its ability to capture the underlying nonlinear relationships among the sequences. The incorporation of hyperbolic geometry in distance calculations allows for a more accurate representation of the data, particularly when dealing with hierarchical or tree-like structures.

Overall, the proposed approach combines the Hyperboloid model with kernel PCA to construct a kernel matrix and derive low-dimensional embeddings. This allows for the exploration and analysis of sequence data in hyperbolic space, facilitating the discovery of hierarchical relationships and capturing nonlinear patterns that may not be fully captured by traditional Euclidean methods.

3.4 Justification of Using Kernel Matrix

Generating a kernel matrix from the Hyperboloid distance offers several technical justifications and benefits:

1. **Nonlinearity:** The Hyperboloid distance is a measure that accounts for the underlying hyperbolic geometry, representing a non-Euclidean space. Through the utilization of this distance, a kernel matrix can be constructed, facilitating the implicit mapping of data into a higher-dimensional feature space. This mapping

enables the capture of intricate and nonlinear relationships, which proves advantageous in scenarios involving hierarchical or tree-like structures commonly found in biological sequences.

2. **Flexibility and Generalization:** The kernel matrix obtained from the distance measure based on the Hyperboloid can be effectively employed with diverse machine learning algorithms designed for kernel matrices. This flexibility enables the application of various techniques, including kernel PCA, kernel SVM, and more. By leveraging these algorithms, we can harness the rich representation capabilities of the kernel matrix to tackle various tasks, such as dimensionality reduction and classification.
3. **Preserving Nonlinear Information:** Kernel PCA applied to the kernel matrix effectively captures the intrinsic nonlinear characteristics of the data, enabling the extraction of low-dimensional embeddings that preserve the underlying structure and patterns. Through the projection of the data onto the principal components, we can retain the discriminative information while reducing the dimensionality. This approach proves valuable for tasks such as data visualization and handling high-dimensional datasets.

4 Experimental Setup

This section outlines the experimental setup, encompassing the utilized dataset, evaluation metrics, and implementation specifics. We present the experimental results, conduct a comparative analysis between the proposed approach and existing methods, and offer a comprehensive interpretation of the findings. All experiments were performed using Python on a system with a Core i5 processor operating at a frequency of 2.4 GHz, 32 GB of memory, and the Windows 10 operating system.

We utilize three real-world biological sequence datasets, consisting of both protein and nucleotide sequences. Table 1 provides a summary of the datasets used in our experiments.

Name	Seq.	Classes	Sequence Statistics			Reference	Description
			Max	Min	Mean		
Spike7k	7000	22	1274	1274	1274.00	[46]	The dataset contains spike protein sequences of the SARS-CoV-2 virus along with information about the coronavirus lineages associated with each sequence.
Human DNA	4380	7	18921	5	1263.59	[47]	The dataset consists of unaligned nucleotide sequences used for classifying the gene family to which humans belong.
Coronavirus Host	5558	21	1584	9	1272.36	ViPR [48], GISAID [46]	The dataset includes spike protein sequences belonging to various clades of the Coronaviridae family, accompanied by labels indicating the infected host (e.g., Humans, Bats, Chickens, etc.).

Table 1: Summary of dataset statistics for the three datasets used in our evaluation.

We have carefully selected a range of recently proposed methods as baselines from various categories of embedding generation. These categories include feature engineering, traditional kernel matrix generation (with kernel PCA), neural networks, pre-trained language models, and pre-trained transformers specifically designed for

protein sequences. Detailed information about these baseline models can be found in Table 2.

Method	Category	Description	Source
PWM2Vec	Feature Engineering	This method takes a biological sequence as input and generates fixed-length numerical embeddings.	[49]
String Kernel	Kernel Matrix	This approach designs an $n \times n$ kernel matrix that can be used with kernel classifiers or kernel PCA to obtain feature vectors based on principal components.	[26]
SeqVec	Pretrained Language Model	This method takes biological sequences as input and fine-tunes the weights based on a pre-trained model to obtain the final embeddings.	[50]
ProteinBERT	Pretrained Transformer	This is a pretrained protein sequence model that utilizes the Transformer/Bert architecture to classify the given biological sequences.	[51]
WDGRL AutoEncoder	Neural Network (NN)	This method takes the one-hot representation of a biological sequence as input and generates embeddings using a neural network by minimizing a loss function.	[52] [53]

Table 2: Description of different baseline models.

To assess the performance of various models, we employ a range of evaluation metrics, including average accuracy, precision, recall, weighted F1 score, macro F1 score, Receiver Operator Characteristic Curve (ROC AUC), and training runtime. For metrics specifically designed for binary classification, we adopt the one-vs-rest approach for multi-class classification. The supervised analysis involves the utilization of both linear and non-linear classifiers. Specifically, we employ: Support Vector Machine (SVM) [54], which finds optimal separating hyperplanes by maximizing the margin between classes; Naive Bayes (NB) [55], a probabilistic classifier based on Bayes' theorem with independence assumptions; Multi-Layer Perceptron (MLP) [56], a feedforward neural network with multiple hidden layers; K-Nearest Neighbors (KNN) [57], an instance-based method that classifies based on majority voting of k nearest neighbors; Random Forest (RF) [58], an ensemble method using multiple decision trees; Logistic Regression (LR) [59], a linear classifier using the logistic function; and Decision Tree (DT) [60], a tree-based rule classifier. For our method, the kernel matrix generated from hyperboloid distances is first processed through kernel PCA to obtain low-dimensional embeddings (as described in Section 3.3). These embeddings are then used as input features to each of the seven classifiers listed above. All classifiers were implemented using scikit-learn [61] with default parameters unless otherwise specified. To visually evaluate if the embeddings generated from the Hyperboloid Model using kernel PCA keep similar points closer to each other in the hyperbolic geometry space, we use the t-Distributed Stochastic Neighbor Embedding (t-SNE) method [62].

4.1 Data Visualization

To visually evaluate if the embeddings generated from the Hyperboloid Model using kernel PCA keep similar points closer to each other in the hyperbolic geometry space, we use the t-Distributed Stochastic Neighbor Embedding (t-SNE) method [62] to get

2-D representations for the embeddings and plot them using the scatterplot. Including t-SNE in this study enables the assessment of the proposed techniques through visual representations of biological sequence classification and grouping, based on their similarities. This visualization is highly valuable in evaluating the effectiveness of the proposed methods in capturing the underlying patterns and relationships within the dataset. The tSNE plots for Spike7k, Human DNA, and Coronavirus Host dataset are shown in Figure 3. For the Spike7k dataset, we can observe that the majority class (i.e., B.1.1.7) and other classes like P.1 and B.1.526 are nicely grouped together. Similarly, for the Human DNA dataset, although we can observe some overlapping of data points belonging to different classes, the classes like Transcription Factor and Synthetase show several smaller groups. Moreover, for the Coronavirus Host dataset, we can observe clear grouping for the classes such as Weasel, Environment, and Turtle. These groupings highlights the fact that the proposed embedding is able to preserve similar classes together in low dimensional representation.

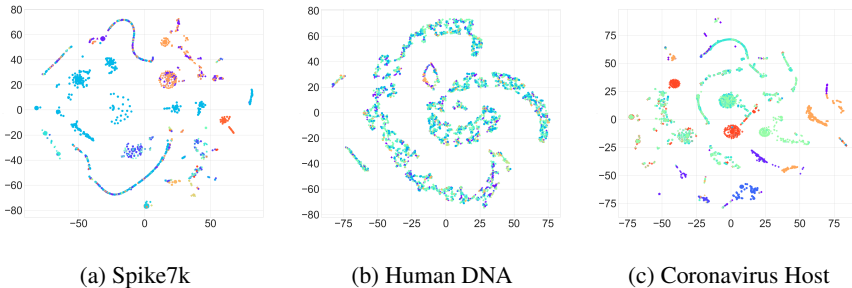


Fig. 3: t-SNE plots for Hyperboloid Model using Spike7k, Human DNA, and Coronavirus Host datasets.

5 Results And Discussion

Table 3 presents the average classification results for the coronavirus host dataset, specifically focusing on spike proteins. Notably, the proposed hyperboloid model-based method outperforms all other methods in terms of average accuracy, precision, recall, and weighted F1 scores. These findings highlight the superior performance of our model in accurately classifying the spike proteins. However, it is worth mentioning that the baseline PWM2Vec method achieves the highest macro F1 macro and ROC-AUC score among all the methods considered while our method achieves comparable performance in this case.

Table 4 presents the classification results (averaged over 5 runs) for the proposed hyperboloid-based method, as well as the baseline models, on the Spike7k dataset. It is evident that the proposed methods consistently outperform the baseline models in terms of predictive performance. These methods consistently achieve higher scores

Embeddings	Algo.	Acc. \uparrow	Prec. \uparrow	Recall \uparrow	F1 (Weig.) \uparrow	F1 (Macro) \uparrow	ROC AUC \uparrow	Train (sec.) \downarrow	Time
PWM2Vec	SVM	0.799	0.806	0.799	0.801	0.648	0.859	44.793	
	NB	0.381	0.584	0.381	0.358	0.400	0.683	<u>2.494</u>	
	MLP	0.782	0.792	0.782	0.778	0.693	0.848	21.191	
	KNN	0.786	0.782	0.786	0.779	0.679	0.838	12.933	
	RF	<u>0.836</u>	<u>0.839</u>	<u>0.836</u>	<u>0.828</u>	0.739	0.862	7.690	
	LR	0.809	0.815	0.809	0.800	0.728	0.852	274.91	
	DT	0.801	0.802	0.801	0.797	0.633	0.829	4.537	
String Kernel	SVM	0.601	0.673	0.601	0.602	0.325	0.624	5.198	
	NB	0.230	0.665	0.230	0.295	0.162	0.625	<u>0.131</u>	
	MLP	0.647	0.696	0.647	0.641	0.302	0.628	42.322	
	KNN	0.613	0.623	0.613	0.612	0.310	0.629	0.434	
	RF	<u>0.668</u>	0.692	<u>0.668</u>	<u>0.663</u>	<u>0.360</u>	<u>0.658</u>	4.541	
	LR	0.554	<u>0.724</u>	0.554	0.505	0.193	0.568	5.096	
	DT	0.646	0.674	0.646	0.643	0.345	0.653	1.561	
WDGRL	SVM	0.329	0.108	0.329	0.163	0.029	<u>0.500</u>	2.859	
	NB	0.004	0.095	0.004	0.007	0.002	0.496	0.008	
	MLP	0.328	0.136	0.328	0.170	0.032	0.499	5.905	
	KNN	0.235	0.198	0.235	0.211	<u>0.058</u>	0.499	0.081	
	RF	0.261	0.196	0.261	<u>0.216</u>	0.051	0.499	1.288	
	LR	<u>0.332</u>	0.149	<u>0.332</u>	0.177	0.034	<u>0.500</u>	0.365	
	DT	0.237	<u>0.202</u>	0.237	0.211	0.054	0.498	0.026	
Autoencoder	SVM	0.602	0.588	0.602	0.590	0.519	0.759	2575.9	
	NB	0.261	0.520	0.261	0.303	0.294	0.673	21.74	
	MLP	0.486	0.459	0.486	0.458	0.216	0.594	29.93	
	KNN	0.763	0.764	0.763	0.755	0.547	0.784	<u>18.51</u>	
	RF	<u>0.800</u>	<u>0.796</u>	<u>0.800</u>	<u>0.791</u>	<u>0.648</u>	<u>0.815</u>	57.90	
	LR	0.717	0.750	0.717	0.702	0.564	0.812	11072.6	
	DT	0.772	0.767	0.772	0.765	0.571	0.808	121.36	
SeqVec	SVM	0.711	0.745	0.711	0.698	0.497	0.747	0.751	
	NB	0.503	0.636	0.503	0.554	0.413	0.648	<u>0.012</u>	
	MLP	0.718	0.748	0.718	0.708	0.407	0.706	10.191	
	KNN	0.815	0.806	0.815	0.809	0.588	0.800	0.418	
	RF	<u>0.833</u>	<u>0.824</u>	<u>0.833</u>	<u>0.828</u>	<u>0.678</u>	<u>0.839</u>	1.753	
	LR	0.673	0.683	0.673	0.654	0.332	0.660	1.177	
	DT	0.778	0.786	0.778	0.781	0.618	0.825	0.160	
Protein Bert	-	0.799	0.806	0.799	0.789	0.715	0.841	15742.9	
Hyperboloid Model (ours)	SVM	0.346	0.261	0.346	0.207	0.040	0.504	13.423	
	NB	0.585	0.633	0.585	0.585	0.460	0.741	<u>0.288</u>	
	MLP	0.751	0.751	0.751	0.746	0.474	0.726	7.102	
	KNN	0.877	0.877	0.877	0.873	0.622	<u>0.832</u>	1.204	
	RF	0.833	0.833	0.833	0.824	<u>0.655</u>	0.810	5.127	
	LR	0.351	0.257	0.351	0.214	0.042	0.505	2.261	
	DT	0.782	0.780	0.782	0.777	0.556	0.790	1.315	

Table 3: Classification results (averaged over 5 runs) for different evaluation metrics for **Coronavirus Host Dataset**. The best values are shown in bold. The best value for each embedding method is shown with the underline.

across various evaluation metrics, demonstrating their superiority compared to other embedding methods.

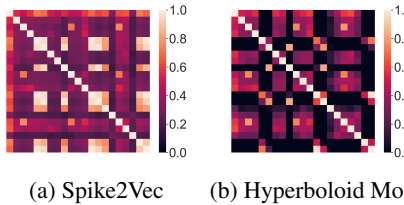
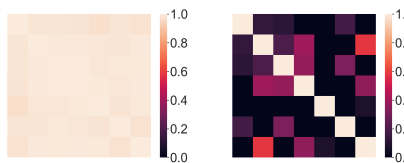


Fig. 4: Heatmap for classes in **Coronavirus Host dataset**.

Embeddings	Algo.	Acc. \uparrow	Prec. \uparrow	Recall \uparrow	F1 (Weig.) \uparrow	F1 (Macro) \uparrow	ROC AUC \uparrow	Train (sec.) \downarrow	Time
PWM2Vec	SVM	0.818	0.820	0.818	0.810	0.606	<u>0.807</u>	22.710	
	NB	0.610	0.667	0.610	0.607	0.218	0.631	1.456	
	MLP	0.812	0.792	0.812	0.794	0.530	0.770	35.197	
	KNN	0.767	0.790	0.767	0.760	0.565	0.773	<u>1.033</u>	
	RF	<u>0.824</u>	<u>0.843</u>	<u>0.824</u>	<u>0.813</u>	<u>0.616</u>	0.803	8.290	
	LR	0.822	0.813	0.822	0.811	0.605	0.802	471.659	
	DT	0.803	0.800	0.803	0.795	0.581	0.791	4.100	
String Kernel	SVM	0.845	0.833	<u>0.846</u>	0.821	0.631	0.812	7.350	
	NB	0.753	0.821	0.755	0.774	0.602	0.825	0.178	
	MLP	0.831	0.829	0.838	0.823	0.624	0.818	12.652	
	KNN	0.829	0.822	0.827	0.827	0.623	0.791	0.326	
	RF	<u>0.847</u>	<u>0.844</u>	0.841	<u>0.835</u>	<u>0.666</u>	0.824	1.464	
	LR	0.845	0.843	0.843	0.826	0.628	0.812	1.869	
	DT	0.822	0.829	0.824	0.829	0.631	0.826	0.243	
WDGRL	SVM	0.792	0.769	0.792	0.772	0.455	0.736	0.335	
	NB	0.724	0.755	0.724	0.726	0.434	0.727	0.018	
	MLP	0.799	0.779	0.799	0.784	0.505	0.755	7.348	
	KNN	<u>0.800</u>	<u>0.799</u>	<u>0.800</u>	<u>0.792</u>	0.546	0.766	0.094	
	RF	0.796	0.793	0.796	0.789	<u>0.560</u>	<u>0.776</u>	0.393	
	LR	0.752	0.693	0.752	0.716	0.262	0.648	0.091	
	DT	0.790	<u>0.799</u>	0.790	0.788	0.557	0.768	<u>0.009</u>	
Autoencoder	SVM	0.699	0.720	0.699	0.678	0.243	0.627	4018.02	
	NB	0.490	0.533	0.490	0.481	0.123	0.620	24.6372	
	MLP	0.663	0.633	0.663	0.632	0.161	0.589	87.4913	
	KNN	0.782	0.791	0.782	0.776	0.535	0.761	<u>24.5597</u>	
	RF	<u>0.814</u>	<u>0.803</u>	0.814	<u>0.802</u>	<u>0.593</u>	<u>0.793</u>	46.583	
	LR	0.761	0.755	0.761	0.735	0.408	0.705	11769.02	
	DT	0.803	0.792	0.803	0.792	0.546	0.779	102.185	
SeqVec	SVM	<u>0.796</u>	0.768	<u>0.796</u>	0.770	0.479	0.747	1.0996	
	NB	0.686	0.703	0.686	0.686	0.351	0.694	<u>0.0146</u>	
	MLP	<u>0.796</u>	0.771	<u>0.796</u>	0.771	0.510	0.762	13.172	
	KNN	0.790	0.787	0.790	<u>0.786</u>	<u>0.561</u>	0.768	0.6463	
	RF	0.793	<u>0.788</u>	0.793	<u>0.786</u>	<u>0.557</u>	<u>0.769</u>	1.8241	
	LR	0.785	0.763	0.785	0.761	0.459	0.740	1.7535	
	DT	0.757	0.756	0.757	0.755	0.521	0.760	0.1308	
Protein Bert	-	0.836	0.828	0.836	0.814	0.570	0.792	14163.52	
Hyperboloid Model (ours)	SVM	0.721	0.660	0.721	0.680	0.172	0.591	4.215	
	NB	0.597	0.783	0.597	0.663	0.531	0.769	0.406	
	MLP	0.751	0.753	0.751	0.747	0.534	0.756	4.896	
	KNN	<u>0.849</u>	<u>0.847</u>	<u>0.849</u>	<u>0.838</u>	<u>0.672</u>	0.824	<u>0.382</u>	
	RF	0.824	0.821	0.824	0.807	0.625	0.791	5.508	
	LR	0.679	0.496	0.679	0.571	0.139	0.563	3.648	
	DT	0.830	0.832	0.830	0.825	0.636	<u>0.835</u>	1.384	

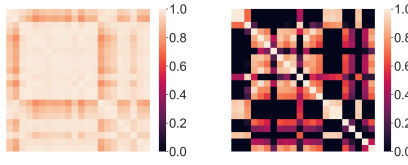
Table 4: Classification results (averaged over 5 runs) on **Spike7k** dataset for different evaluation metrics. The best values are shown in bold. The best value for each embedding method is shown with the underline.



(a) Spike2Vec (b) Hyperboloid Model

Fig. 5: Heatmap for classes in **Human DNA dataset**.

The classification results for the Human DNA dataset are summarized in Table 5, representing the average performance across multiple evaluation metrics. Notably, the proposed hyperboloid model demonstrates superior performance compared to all



(a) Spike2Vec (b) Hyperboloid Model

Fig. 6: Heatmap for classes in **Spike7k** dataset.

other methods, achieving higher average accuracy, recall, weighted F1, macro F1, and ROC-AUC scores. These results highlight the effectiveness of the proposed kernel method in distinguishing between biological sequences, surpassing the performance of the baselines.

An interesting observation is the poor performance of the pre-trained Protein Bert model on the Human DNA dataset compared to its performance on the other two datasets. This discrepancy can be attributed to the fact that Protein Bert is specifically trained on protein sequence data, while the Human DNA dataset consists of nucleotide sequences. Hence the Protein Bert failed to generalize effectively in this case. In contrast, the proposed method exhibits superior performance compared to the baseline models, emphasizing their effectiveness in handling the Human DNA dataset.

5.1 Statistical Analysis

To assess the statistical significance of the results, the student t-test was conducted using the average values and standard deviations (SD) from 5 runs. The SD values for all metrics were found to be very small i.e. < 0.002 . Hence, the majority of the computed p-values were less than 0.05, indicating the statistical significance of the results.

5.2 Inter-Class Embedding Interaction

We utilize heat maps to analyze further whether our proposed kernel can identify different classes better. These maps are generated by first taking the average of the similarity values to compute a single value for each pair of classes and then computing the pairwise cosine similarity of different class's embeddings with one another. The heat map is further normalized between [0-1] to the identity pattern. The heatmaps for the baseline and its comparison with the proposed method embeddings are reported in Figure 4, 5 and 6. We can observe that in the case of the data heatmap, the embeddings for the label are towards similar side. This eventually means it is difficult to distinguish between different classes due to high pairwise similarities among their vectors. On the other hand, we can observe that the pairwise similarity between different class embeddings is distinguishable for proposed method embeddings. This essentially means that the embeddings that belong to similar classes are highly similar to each other. In contrast, the embeddings for different classes are very different,

Embeddings	Algo.	Acc. \uparrow	Prec. \uparrow	Recall \uparrow	F1 (Weig.) \uparrow	F1 (Macro) \uparrow	ROC AUC \uparrow	Train (sec.) \downarrow	Time
PWM2Vec	SVM	0.302	0.241	0.302	0.165	0.091	0.505	10011.3	
	NB	0.084	<u>0.442</u>	0.084	0.063	0.066	<u>0.511</u>	4.565	
	MLP	<u>0.310</u>	0.350	<u>0.310</u>	0.175	0.107	0.510	320.555	
	KNN	0.121	0.337	0.121	0.093	0.077	0.509	2.193	
	RF	0.309	0.332	0.309	<u>0.181</u>	0.110	0.510	65.250	
	LR	0.304	0.257	0.304	0.167	0.094	0.506	23.651	
String Kernel	DT	0.306	0.284	0.306	<u>0.181</u>	<u>0.111</u>	0.509	<u>1.861</u>	
	SVM	0.618	0.617	0.618	0.613	0.588	0.753	39.791	
	NB	0.338	0.452	0.338	0.347	0.333	0.617	<u>0.276</u>	
	MLP	0.597	0.595	0.597	0.593	0.549	0.737	331.068	
	KNN	0.645	0.657	0.645	0.646	0.612	0.774	1.274	
	RF	<u>0.731</u>	<u>0.776</u>	<u>0.731</u>	<u>0.729</u>	<u>0.723</u>	<u>0.808</u>	12.673	
WDGRL	LR	0.571	0.570	0.571	0.558	0.532	0.716	2.995	
	DT	0.630	0.631	0.630	0.630	0.598	0.767	2.682	
	SVM	0.318	0.101	0.318	0.154	0.069	0.500	0.751	
	NB	0.232	0.214	0.232	0.196	0.138	0.517	<u>0.004</u>	
	MLP	0.326	0.286	0.326	0.263	0.186	0.535	8.613	
	KNN	0.317	0.317	0.317	0.315	0.266	0.574	0.092	
Autoencoder	RF	<u>0.453</u>	<u>0.501</u>	<u>0.453</u>	<u>0.430</u>	<u>0.389</u>	<u>0.625</u>	1.124	
	LR	0.323	0.279	0.323	0.177	0.095	0.507	0.041	
	DT	0.368	0.372	0.368	0.369	0.328	0.610	0.047	
	SVM	0.621	0.638	0.621	0.624	0.593	0.769	22.230	
	NB	0.260	0.426	0.260	0.247	0.268	0.583	0.287	
	MLP	0.621	0.624	0.621	0.620	0.578	0.756	111.809	
SeqVec	KNN	0.565	0.577	0.565	0.568	0.547	0.732	1.208	
	RF	0.689	0.738	0.689	0.683	0.668	0.774	20.131	
	LR	<u>0.692</u>	<u>0.700</u>	<u>0.692</u>	<u>0.693</u>	<u>0.672</u>	<u>0.799</u>	58.369	
	DT	0.543	0.546	0.543	0.543	0.515	0.718	10.616	
	SVM	0.656	0.661	0.656	0.652	0.611	<u>0.791</u>	0.891	
	NB	0.324	0.445	0.312	0.295	0.282	0.624	<u>0.036</u>	
Hyperboloid Model (ours)	MLP	0.657	0.633	0.653	0.646	0.616	0.783	12.432	
	KNN	0.592	0.606	0.592	0.591	0.552	0.717	0.571	
	RF	0.713	<u>0.724</u>	0.701	0.702	<u>0.693</u>	0.752	2.164	
	LR	<u>0.725</u>	0.715	0.726	<u>0.725</u>	0.685	0.784	1.209	
	DT	0.586	0.553	0.585	0.577	0.557	0.736	0.24	
	Protein Bert	-	0.542	0.580	0.542	0.514	0.447	0.675	58681.57
	SVM	0.508	0.441	0.508	0.458	0.357	0.642	8.440	
	NB	0.260	0.320	0.260	0.236	0.200	0.553	<u>0.101</u>	
	MLP	0.574	0.580	0.574	0.575	0.544	0.736	4.265	
	KNN	0.739	0.748	0.739	0.740	0.724	0.836	2.339	
	RF	0.687	0.770	0.687	0.686	0.689	0.779	3.621	
	LR	0.488	0.437	0.488	0.429	0.338	0.627	0.790	
	DT	0.583	0.586	0.583	0.583	0.545	0.739	1.256	

Table 5: Classification results (averaged over 5 runs) on **Human DNA** dataset for different evaluation metrics. The best values are shown in bold. The best value for each embedding method is shown with the underline.

indicating that the proposed methodology can accurately identify similar classes and different classes.

The obtained results indicate that the proposed method consistently outperforms all baseline methods across different datasets in terms of average classification performance. This demonstrates the generalizability of the proposed approach, as it achieves higher predictive accuracy on both protein and nucleotide datasets. Furthermore, compared to the traditional String kernel method, the proposed approach exhibits superior performance, emphasizing its effectiveness in preserving information in the higher-dimensional space by capturing hierarchical and structural information. Additionally, the statistical significance of the results on real-world biological sequence datasets is demonstrated.

6 Conclusion

In this study, we introduced a novel approach for the analysis of biological sequences by transforming their feature representation into the hyperboloid space. By leveraging this transformation, the proposed method preserved the hierarchical and structural information inherent in the sequences, addressing the limitations of conventional machine learning approaches operating in the Euclidean spaces. The experimental evaluation showcased the efficacy of the proposed approach in capturing important sequence correlations and improving classification accuracy. We also provide theoretical detail regarding the important kernel properties. Furthermore, the statistical significance of the results was confirmed through the student t-test. Future research directions involve exploring the applications of the hyperboloid space in other areas of bioinformatics and investigating its performance on larger and more diverse biological datasets.

7 Funding

Not Applicable

8 Conflicts of interest/Competing interests

The authors do not have any conflict of interest

9 Ethics approval

Not Applicable

10 Consent to participate

Not Applicable

11 Consent for publication

Not Applicable

12 Availability of data and material

Available on request

13 Code availability

Available on request

14 Authors' contributions

S. Ali and H. Mansoor worked on algorithm design. S. Ali performed experiments. H. Mansoor worked on theoretical analysis. M. Patterson supervised the project. All authors wrote and reviewed the manuscript

References

- [1] Koonin, E., Galperin, M.Y.: Sequence—evolution—function: computational approaches in comparative genomics (2002)
- [2] Tayebi, Z., Ali, S., Murad, T., Khan, I., Patterson, M.: Pseaac2vec protein encoding for tcr protein sequence classification. *Computers in Biology and Medicine* **170**, 107956 (2024)
- [3] Tillquist, R.C.: Low-dimensional embeddings for symbolic data science. PhD thesis, University of Colorado at Boulder (2020)
- [4] Bhattacharjya, A.K., Ancin, H.: Data embedding in text for a copier system. In: Proceedings 1999 International Conference on Image Processing (Cat. 99CH36348), vol. 2, pp. 245–249 (1999). IEEE
- [5] Cai, H., Zheng, V.W., Chang, K.C.-C.: A comprehensive survey of graph embedding: Problems, techniques, and applications. *IEEE transactions on knowledge and data engineering* **30**(9), 1616–1637 (2018)
- [6] Pezeshkpour, P., Chen, L., Singh, S.: Embedding multimodal relational data for knowledge base completion. *arXiv preprint arXiv:1809.01341* (2018)
- [7] Harder, T.C., Kenter, M., Vos, H., Siebelink, K., Huisman, W., Van Amerongen, G., Örvell, C., Barrett, T., Appel, M., Osterhaus, A.: Canine distemper virus from diseased large felids: biological properties and phylogenetic relationships. *Journal of General Virology* **77**(3), 397–405 (1996)
- [8] Nakagawa, H., Fujita, M.: Whole genome sequencing analysis for cancer genomics and precision medicine. *Cancer science* **109**(3), 513–522 (2018)
- [9] Eisenhaber, F., Persson, B., Argos, P.: Protein structure prediction: recognition of primary, secondary, and tertiary structural features from amino acid sequence. *Critical reviews in biochemistry and molecular biology* **30**(1), 1–94 (1995)
- [10] Fagan, M.J., Saier, M.H.: P-type atpases of eukaryotes and bacteria: sequence analyses and construction of phylogenetic trees. *Journal of molecular evolution* **38**, 57–99 (1994)
- [11] Kuzmin, K., Adeniyi, A.E., DaSouza Jr, A.K., Lim, D., Nguyen, H., Molina,

N.R., Xiong, L., Weber, I.T., Harrison, R.W.: Machine learning methods accurately predict host specificity of coronaviruses based on spike sequences alone. *Biochemical and Biophysical Research Communications* **533**(3), 553–558 (2020)

[12] Ali, S., Patterson, M.: Spike2vec: An efficient and scalable embedding approach for covid-19 spike sequences. In: *IEEE International Conference on Big Data (Big Data)*, pp. 1533–1540 (2021)

[13] Chourasia, P., Ali, S., Ciccolella, S., Vedova, G.D., Patterson, M.: Reads2vec: Efficient embedding of raw high-throughput sequencing reads data. *Journal of Computational Biology* **30**(4), 469–491 (2023)

[14] Chourasia, P., Murad, T., Ali, S., Patterson, M.: Enhancing t-sne performance for biological sequencing data through kernel selection. In: *International Symposium on Bioinformatics Research and Applications*, pp. 442–452 (2023). Springer

[15] Ali, S., Ali, T.E., Chourasia, P., Patterson, M.: Compression and k-mer based approach for anticancer peptide analysis. *bioRxiv*, 2024–10 (2024)

[16] Taslim, M., Prakash, C., Sarwan, A., Murray, P.: Hashing2vec: Fast embedding generation for sars-cov-2 spike sequence classification. In: *Asian Conference on Machine Learning*, pp. 754–769 (2023). PMLR

[17] Ali, S., Sahoo, B., Ullah, N., Zelikovskiy, A., Patterson, M., Khan, I.: A k-mer based approach for SARS-CoV-2 variant identification. In: *International Symposium on Bioinformatics Research and Applications*, pp. 153–164 (2021)

[18] Asim, M.N., Malik, M.I., Dengel, A., Ahmed, S.: K-mer neural embedding performance analysis using amino acid codons. In: *2020 International Joint Conference on Neural Networks (IJCNN)*, pp. 1–8 (2020). IEEE

[19] Ali, S., Mansoor, H., Chourasia, P., Ali, Y., Patterson, M.: Gaussian beltrami-klein model for protein sequence classification: A hyperbolic approach. In: *International Symposium on Bioinformatics Research and Applications*, pp. 52–62 (2024). Springer

[20] Ali, S., Ali, T.E., Murad, T., Mansoor, H., Patterson, M.: Molecular sequence classification using efficient kernel based embedding. *Information Sciences* **679**, 121100 (2024)

[21] Ali, S., Mansoor, H., Chourasia, P., Khan, I.U., Patterson, M.: Preserving hidden hierarchical structure: Poincaré distance for enhanced genomic sequence analysis. In: *Annual International Conference on Information Management and Big Data*, pp. 3–19 (2024). Springer

- [22] Ali, S., Shabbir, M., Mansoor, H., Chourasia, P., Patterson, M.: Elliptic geometry-based kernel matrix for improved biological sequence classification. *Knowledge-Based Systems* **304**, 112479 (2024)
- [23] Ali, S., Ali, T.E., Patterson, M.: Hash-binding: Dna-protein binding prediction using hashing-based embedding. *Neural Computing and Applications*, 1–36 (2025)
- [24] Ali, S., Ali, T.E., Mansoor, H., Chourasia, P., Patterson, M.: Hist2vec: A histogram and kernel-based embedding method for molecular sequence analysis. *Expert Systems with Applications* **273**, 126859 (2025)
- [25] Murad, T., Ali, S., Patterson, M.: Sequence analysis using the bezier curve. arXiv preprint arXiv:2503.14574 (2025)
- [26] Ali, S., Sahoo, B., Khan, M.A., Zelikovsky, A., Khan, I.U., Patterson, M.: Efficient approximate kernel based spike sequence classification. *IEEE/ACM Transactions on Computational Biology and Bioinformatics* (2022)
- [27] Ho, S.Y., Jermiin, L.S.: Tracing the decay of the historical signal in biological sequence data. *Systematic biology* **53**(4), 623–637 (2004)
- [28] Chappell, T., Geva, S., Hogan, J.: K-means clustering of biological sequences. In: *Proceedings of the 22nd Australasian Document Computing Symposium*, pp. 1–4 (2017)
- [29] Deshpande, M., Karypis, G.: Evaluation of techniques for classifying biological sequences. In: *Advances in Knowledge Discovery and Data Mining: 6th Pacific-Asia Conference, PAKDD 2002 Taipei, Taiwan, May 6–8, 2002 Proceedings*, pp. 417–431 (2002). Springer
- [30] Kimothi, D., Soni, A., Biyani, P., Hogan, J.M.: Distributed representations for biological sequence analysis. arXiv preprint arXiv:1608.05949 (2016)
- [31] Iuchi, H., Matsutani, T., Yamada, K., Iwano, N., Sumi, S., Hosoda, S., Zhao, S., Fukunaga, T., Hamada, M.: Representation learning applications in biological sequence analysis. *Computational and Structural Biotechnology Journal* **19**, 3198–3208 (2021)
- [32] Corso, G., Ying, Z., Pándy, M., Veličković, P., Leskovec, J., Liò, P.: Neural distance embeddings for biological sequences. *Advances in Neural Information Processing Systems* **34**, 18539–18551 (2021)
- [33] Liu, J., Wang, W.: Op-cluster: Clustering by tendency in high dimensional space. In: *Third IEEE International Conference on Data Mining*, pp. 187–194 (2003). IEEE

- [34] Ali, S.: Evaluating covid-19 sequence data using nearest-neighbors based network model. In: IEEE International Conference on Big Data (Big Data), pp. 5182–5188 (2022)
- [35] Tsai, C.-J., Ma, B., Nussinov, R.: Protein–protein interaction networks: how can a hub protein bind so many different partners? *Trends in biochemical sciences* **34**(12), 594–600 (2009)
- [36] Kimothi, D., Shukla, A., Biyani, P., Anand, S., Hogan, J.M.: Metric learning on biological sequence embeddings. In: 2017 IEEE 18th International Workshop on Signal Processing Advances in Wireless Communications (SPAWC), pp. 1–5 (2017). IEEE
- [37] Tayebi, Z., Ali, S., Patterson, M.: Tcellr2vec: efficient feature selection for tcr sequences for cancer classification. *PeerJ Computer Science* **10**, 2239 (2024)
- [38] Tayebi, Z., Ali, S., Chourasia, P., Murad, T., Patterson, M.: T cell receptor protein sequences and sparse coding: A novel approach to cancer classification. In: International Conference on Neural Information Processing, pp. 215–227 (2023). Springer
- [39] Tayebi, Z., Ali, S., Patterson, M.: Robust representation and efficient feature selection allows for effective clustering of SARS-CoV-2 variants. *Algorithms* **14**(12), 348 (2021)
- [40] Hoffmann, H.: Kernel PCA for novelty detection. *Pattern recognition* **40**(3), 863–874 (2007)
- [41] Nickel, M., Kiela, D.: Poincaré embeddings for learning hierarchical representations. *Advances in neural information processing systems* **30** (2017)
- [42] Chen, B., Huang, X., Xiao, L., Cai, Z., Jing, L.: Hyperbolic interaction model for hierarchical multi-label classification. In: Proceedings of the AAAI Conference on Artificial Intelligence, vol. 34, pp. 7496–7503 (2020)
- [43] Park, J., Cho, J., Chang, H.J., Choi, J.Y.: Unsupervised hyperbolic representation learning via message passing auto-encoders. In: Proceedings of the IEEE/CVF Conference on Computer Vision and Pattern Recognition, pp. 5516–5526 (2021)
- [44] Sala, F., De Sa, C., Gu, A., Ré, C.: Representation tradeoffs for hyperbolic embeddings. In: International Conference on Machine Learning, pp. 4460–4469 (2018). PMLR
- [45] Xu, Y., Ye, Q.: Generalized Mercer Kernels and Reproducing Kernel Banach Spaces vol. 258, (2019)

- [46] GISAID Website <https://www.gisaid.org/>. [Online; accessed 17-December-2022] (2022)
- [47] Human DNA <https://www.kaggle.com/code/nageshsingh/demystify-dna-sequencing-with-machine-learning/data>. [Online; accessed 10-October-2022]
- [48] Pickett, B.E., Sadat, E.L., Zhang, Y., Noronha, J.M., Squires, R.B., Hunt, V., Liu, M., Kumar, S., Zaremba, S., Gu, Z., *et al.*: Vipr: an open bioinformatics database and analysis resource for virology research. *Nucleic acids research* **40**(D1), 593–598 (2012)
- [49] Ali, S., Bello, B., Chourasia, P., Punathil, R.T., Zhou, Y., Patterson, M.: PWM2Vec: An efficient embedding approach for viral host specification from coronavirus spike sequences. *Biology* **11**(3), 418 (2022)
- [50] Heinzinger, M., Elnaggar, A., Wang, Y., Dallago, C., Nechaev, D., Matthes, F., Rost, B.: Modeling aspects of the language of life through transfer-learning protein sequences. *BMC bioinformatics* **20**(1), 1–17 (2019)
- [51] Brandes, N., Ofer, D., Peleg, Y., Rappoport, N., Linial, M.: Proteinbert: A universal deep-learning model of protein sequence and func. *Bioinformatics* **38**(8) (2022)
- [52] Shen, J., Qu, Y., Zhang, W., Yu, Y.: Wasserstein distance guided representation learning for domain adaptation. In: AAAI Conference on Artificial Intelligence (2018)
- [53] Xie, J., Girshick, R., Farhadi, A.: Unsupervised deep embedding for clustering analysis. In: International Conference on Machine Learning, pp. 478–487 (2016)
- [54] Cortes, C., Vapnik, V.: Support-vector networks. *Machine learning* **20**(3), 273–297 (1995)
- [55] Rish, I., *et al.*: An empirical study of the naive bayes classifier. In: IJCAI 2001 Workshop on Empirical Methods in Artificial Intelligence, vol. 3, pp. 41–46 (2001). Seattle, USA
- [56] Gardner, M.W., Dorling, S.R.: Artificial neural networks (the multilayer perceptron)—a review of applications in the atmospheric sciences. *Atmospheric environment* **32**(14–15), 2627–2636 (1998)
- [57] Cover, T., Hart, P.: Nearest neighbor pattern classification. *IEEE transactions on information theory* **13**(1), 21–27 (1967)
- [58] Breiman, L.: Random forests. *Machine learning* **45**(1), 5–32 (2001)

- [59] Hosmer, D.W., Lemeshow, S., et al.: Applied logistic regression. john wiley & sons. New York (2000)
- [60] Quinlan, J.R.: Induction of decision trees. *Machine learning* **1**(1), 81–106 (1986)
- [61] Pedregosa, F., Varoquaux, G., Gramfort, A., Michel, V., Thirion, B., Grisel, O., Blondel, M., Prettenhofer, P., Weiss, R., Dubourg, V., et al.: Scikit-learn: Machine learning in python. *the Journal of machine Learning research* **12**, 2825–2830 (2011)
- [62] Van der M., L., Hinton, G.: Visualizing data using t-SNE. *Journal of Machine Learning Research (JMLR)* **9**(11) (2008)